

Binding fullereneol $C_{60}(OH)_{24}$ to dsDNA

Mariana Pinteala
Andrei Dascalu
Cezar Ungurenasu

Petru Poni Institute of
Macromolecular Chemistry,
Aleea Grigore Ghica,
Iasi, Romania

Abstract: The first $C_{60}(OH)_{24}$ -DNA complex and its fluorescence enhancement is reported. The enhanced fluorescence intensity of fullereneol $C_{60}(OH)_{24}$ is in proportion to the concentration of DNA in the range of 1×10^{-9} to 8×10^{-5} molL⁻¹ and the detection limit was 1.3 ng mL⁻¹. Fullereneol $C_{60}(OH)_{24}$ binds significantly to the phosphate backbone of native dsDNA and to base-pairs within the major groove of sodium salt of dsDNA.

Keywords: nanomedicine, fullereneol, DNA complexation, fluorescent probe

Introduction

Nanoscale materials seems to offer great opportunities for biomedical applications such as therapeutic and diagnostic tools.¹⁻⁹ Biomedical applications under development include drug delivery systems targeted to the brain and cancer tissues, gene transfection, and intravascular nanosensor and nanorobotic devices for imaging and diagnosis.^{3,9}

In this context, the biological activities of fullerene derivatives have attracted much attention in the past 25 years.¹⁰⁻¹⁷ As potent free-radical scavengers and antioxidants¹⁸⁻²³ the water-soluble polyhydroxylated [C_{60}]fullerenes, fullereneols, exhibit an exciting range of biological activities as glutamate receptor antagonists,²⁴ antiproliferative,²⁵⁻²⁷ neuroprotective,²⁸⁻³¹ and anticancer agents.³²⁻³⁷

Knowing the ways fullereneols interact with proteins and nucleotides is a prerequisite for understanding their biological effects at membrane penetration and the intracellular level, only two studies deal with their binding to proteins^{38,39} and their interaction with DNA has not been reported to date.

On the other hand, the solution-based assays and quantitative analysis of nucleic acids are critical in current biochemistry and biomedical science. Throughout the years, a number of fluorimetric methods for the determination of nucleic acids have been developed with ethidium bromide,⁴⁰⁻⁴² lanthanide cations,⁴³⁻⁴⁵ ruthenium complexes,⁴⁶⁻⁴⁸ and asymmetric cyanine dyes as fluorescence probes.⁴⁹⁻⁵¹

Despite the prominence of fullerenes in bionanotechnology, the exploration of their fluorescent properties in solution remains still at a very early age. Several studies have been devoted to dsDNA/single-walled carbon nanotube hybrid systems,^{52,53} but only very few deal with their fluorescent properties^{54,55} when dispersed in aqueous solution.

Herein, we are happy to report the first complexation of dsDNA with $C_{60}(OH)_{24}$ in aqueous media in the absence of a buffer in physiological pH-range.

Correspondence: Cezar Ungurenasu
Petru Poni Institute of Macromolecular
Chemistry, Aleea Grigore Ghica Voda
41 A, 700487 Iasi, Romania
Email cezar_u@yahoo.com

Materials and methods

C_{60} (99.5+%) was purchased from MER Corp (Tucson, AZ, USA). KOH (99.99%, semiconductor grade) was purchased from Sigma-Aldrich (St. Louis, MO, USA). DNA (low molecular weight, salmon sperm) was purchased from Fluka (St. Louis, MO, USA). All other reagents were purchased from Sigma-Aldrich.

Fluorescence spectroscopy was performed with a Perkin Elmer LS55 spectrometer Perkin Elmer, Wellesley, MA, USA). To prepare fluorescence samples, the only operation was the mixing of two solutions before fluorescence measurements. X-ray photoelectron spectroscopy (XPS) measurements were carried out using a Leybold LHS 10 spectrometer (Leybold, Cologne, Germany).

To the best of our knowledge, most of these fullerlenols are not pure $C_{60}(OH)_n$, but a complex mixture of products. For instance, those synthesized through sulfuric/nitric acid,⁵⁶ hydroboration,⁵⁷ or nitronium chemistry⁵⁸ afforded products with average composition of $C_{60}O_x(OH)_y$. The so-called fullerlenols prepared by alkaline polyhydroxylation of C_{60} under phase transfer conditions⁵⁹ are not simply $C_{60}(OH)_x$, but stable radical anions with the molecular formula, $Na^+[C_{60}O_x(OH)_y]^{n-}$,⁶⁰ and the fullerlenol obtained by alkaline hydrolysis of $C_{60}Br_{24}$ is not $C_{60}(OH)_{24}$ as claimed by Bogdanovi and Dvordjevic,^{37,61} but $C_{60}(ONa)_8(OH)_{16}$.⁶² In the light of this, many biomedical studies involving fullerlenols species in the literature may need to be reconsidered. The pure fullerlenol $C_{60}(OH)_{24}$ used in this study was prepared by a modified method of alkaline hydrolysis of $C_{60}Br_{24}$,⁶² followed by demetallation of the obtained $C_{60}(OK)_8(OH)_{16}$ with a cation exchange resin and exhaustive purification by dialysis.

Representative procedure for synthesis of $C_{60}(OH)_{24}$

All experiments were performed with Schlenk techniques under argon and protected from light. According to the literature, before the synthesis of the polyhydroxylated fullerene, bromofullerene $C_{60}Br_{24}$ was synthesized first.⁶² In the synthesis of the $C_{60}(OH)_{24}$, to a sonicated (40 W, 15 min) suspension of $C_{60}Br_{24}$ (200 mg, 0.075 mmol) in de-aerated water (100 mL), fresh KOH (200 mg, 3.57 mmol) was added under argon protection and stirred for 10 days at room temperature. After the reaction was completed, the resulting dark-brown solution was passed to a centrifuge at 4000 rpm for 30 min and the supernatant was brought to dryness in a rotavapor apparatus at 40 °C. The dark-brown residue was dissolved in 50 mL of deionized water, stirred

with ion exchange resin AMBERJET™ 1200[H] (Rohm and Haas Company, Philadelphia, PA, USA) (20 mL) for 8 h and subjected to dialysis (Spectra/Por® 1000 D; Spectrum Laboratories, Rancho Dominguez, CA, USA) for four days. Finally, the dialyzed solution was brought to dryness in a rotavapor apparatus at 60 °C and dried at 80 °C and 10^{-4} Torr for 24 h. The fullerlenol thus obtained contained 24 hydroxyl groups as characterized by elemental analysis, Fourier transform infrared (FT-IR) spectroscopy, and XPS spectroscopic measurements.

Elemental analysis

Calculated for $C_{60}H_{24}O_{24}$: C, 63.82; H, 2.12. Found: C, 63.66; H, 1.98. FTIR (KBr): ν max, 3436 (–OH), 1605 (C = C), 1430 (δ –OH), 1095, 1046 (ν C–OH), 1018, 994, 825, 877, 570, 530 cm^{-1} .

XPS analysis

C1s components: % C = C (284.6 eV) 59.77 (clcd. 60); % C–OH: (285.8 eV) 39.76 (clcd. 40); O/C = 0.42 (clcd. 0.40).

Results and discussion

The fullerlenol water solution, exhibited different maxima depending on the concentration (Figure 1a). In the range of 1.6×10^{-5} to 4.4×10^{-5} molL⁻¹ one fluorescent maximum was observed at 469 nm, while two fluorescence maxima were found for lower concentrations located at 469 nm and 492 nm at $\lambda_{ex} = 420$ nm.

These emission profiles of fullerlenol at different concentrations provided the baseline for understanding perturbation upon interaction with dsDNA. As shown in Figure 1a, the most appropriate concentrations of fullerlenol in water for fluorescence measurements at $\lambda_{ex} = 420$ nm are within the range of 1.6×10^{-5} to 4.4×10^{-5} molL⁻¹ ($\lambda_{em} = 469$ nm).

As can be seen from Figure 1b, the fluorescence intensity of fullerlenol alone is dependent on its concentration in the range of 4.4×10^{-5} to 1.6×10^{-5} molL⁻¹ according to a very significant linear relationship.

Figure 2 shows the fullerlenol and DNA emission spectra recorded at different excitation wavelengths. Inspection of how fluorescence emission spectra of fullerlenol and DNA change as a function of excitation wavelength yield additional supporting information on the appropriate fullerlenol excitation wavelength suitable for the fluorescence investigation of $C_{60}(OH)_{24}$ –DNA complex in aqueous media. One can observe that for a concentration higher than 1.6×10^{-5} molL⁻¹, the emission spectra of fullerlenol do not overlap with emission spectra of DNA when excited at 340, 360, 380, and

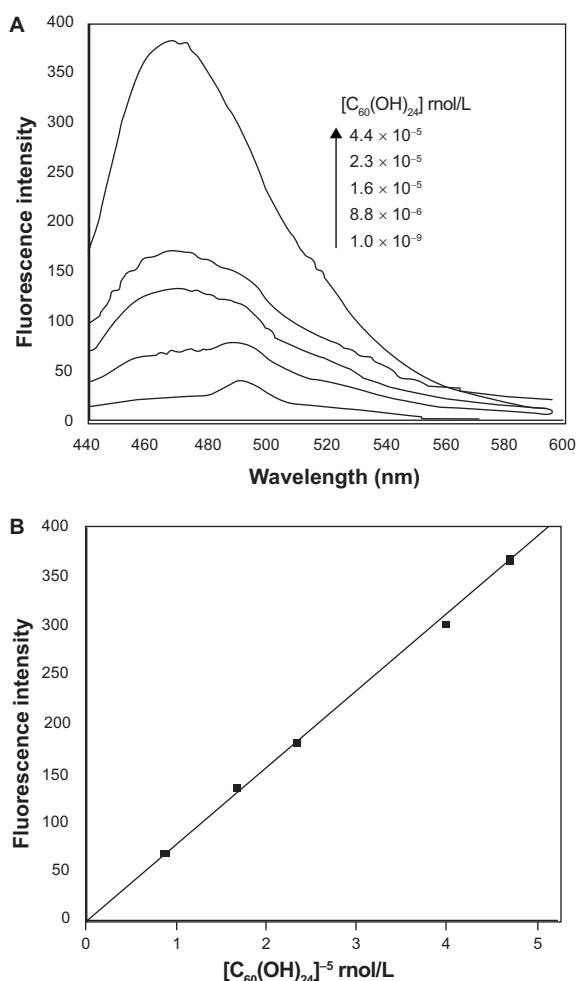


Figure 1 Fluorescence data of $C_{60}(OH)_{24}$ in aqueous media. **A)** Fluorescence emission spectra of $C_{60}(OH)_{24}$ after 5 min incubation in water, with excitation at 420 nm. **B)** Plot of fluorescence intensity versus $[C_{60}(OH)_{24}]^5$, with excitation at 420 nm; average standard error, 3.76%.

420 nm, respectively. Apparently, all these fluorescence excitations should be suitable for a fluorescence study of DNA-fullereneol interaction. However, the emission maxima of fullereneol at concentrations $< 1.6 \times 10^{-5} \text{ molL}^{-1}$ (Figure 1a) and DNA (Figure 2a) overlap at 492 nm when recorded at $\lambda_{\text{ex}} = 420 \text{ nm}$. This is the reason why, to cover a large concentration range (1^{-9} – $4.5^{-5} \text{ molL}^{-1}$) of fullereneol, the fluorescence excitation at 420 nm and emission at 469 nm were used for fluorescence intensity measurements in this work.

In Figure 3a, the emission spectra of DNA-fullereneol complexes, with constant DNA concentration and increasing fullereneol content are shown. It can be seen that increasing the concentration of the fullereneol results in a strong increase in fluorescence intensity of fullereneol from 50 to 500 nm, without causing any perceptible shifts of the fluorescence maximum at $\lambda = 469 \text{ nm}$. In order to establish the DNA binding affinity of fullereneol, these fluorescent-enhancing

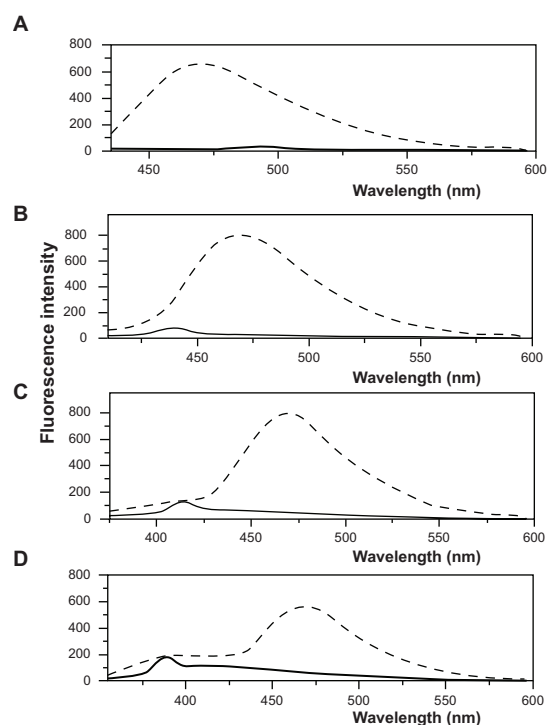
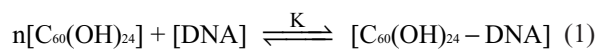


Figure 2 Fluorescence emission spectra of fullereneol (---) and dsDNA (—) for different excitation wavelength. **A)** $\lambda = 420 \text{ nm}$. **B)** $\lambda = 380 \text{ nm}$. **C)** $\lambda = 360 \text{ nm}$. **D)** $\lambda = 340 \text{ nm}$. $[C_{60}(OH)_{24}] = 1 \times 10^{-4} \text{ molL}^{-1}$; $[DNA] = 1 \times 10^{-4} \text{ molL}^{-1}$.

data were plotted (Figure 3b) according to the equation (6) derived from the equilibrium equation (1):



$$K = \frac{[C_{60}(OH)_{24} - DNA]}{[C_{60}(OH)_{24}]^n [DNA]} \quad (2)$$

$$[C_{60}(OH)_{24} - DNA] = K[C_{60}(OH)_{24}]^n [DNA] \quad (3)$$

$$\log [C_{60}(OH)_{24} - DNA] = \log K + n \log [C_{60}(OH)_{24}] + \log [DNA] \quad (4)$$

$$\log \frac{[C_{60}(OH)_{24} - DNA]}{[DNA]} = \log K + n \log [C_{60}(OH)_{24}] \quad (5)$$

$$\log \frac{F - F_1}{F_0} = \log K + n \log [C_{60}(OH)_{24}] \quad (6)$$

where F_1 is the fluorescence intensity from the fullereneol in the absence of DNA (Figure 1b), F_0 is the fluorescence intensity from the DNA in the absence of fullereneol at 467 nm for $\lambda_{\text{ex}} = 420 \text{ nm}$ (Figure 2a), F is the fluorescence intensity from the DNA-fullereneol complex in the presence of different concentrations of the fullereneol (Figure 3b) and n is the number of associated molecules of fullereneol with one base pair of DNA. From the linear plot for $(\log(F - F_1)/F_0)$ vs $(\log[C_{60}(OH)_{24}])$ (Figure 5), according to equation (1), the values of K and n were estimated to be $6 \times 10^5 \text{ M}^{-1}$ and 0.8 ± 0.2 , respectively.

In order to evaluate the range of $[DNA]$ determination, the binding of fullereneol to DNA was characterized

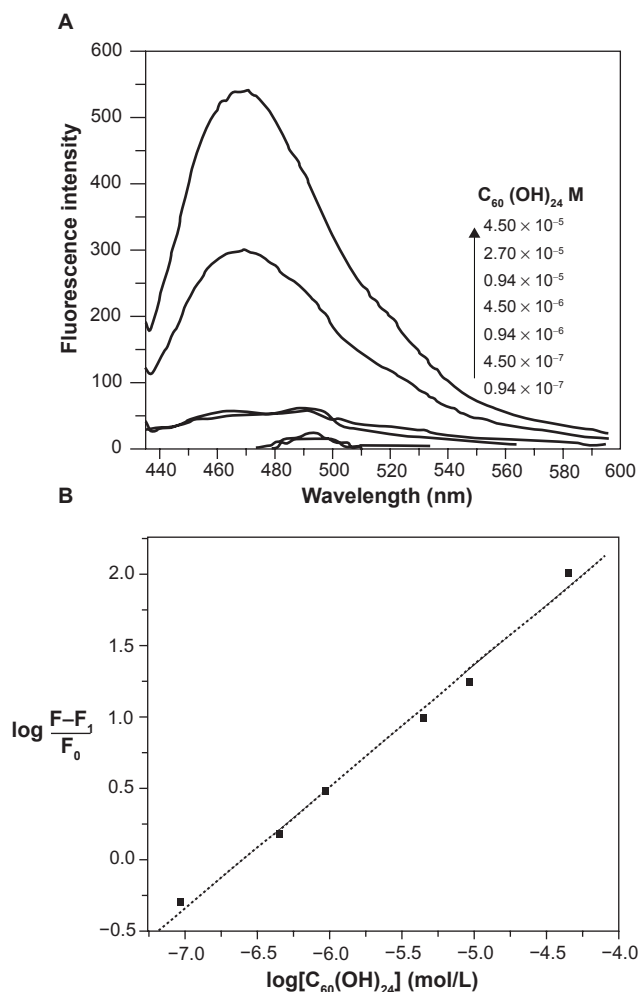


Figure 3 Fluorescence data of $C_{60}(OH)_{24}$ in the presence of dsDNA. **A**) Fluorescence emission spectra of fullereneol (—) in the presence of dsDNA (---) with excitation at 420 nm, as a function of fullereneol concentration; [dsDNA] = 6.31×10^{-5} mol/L. **B**) Plot for DNA- $C_{60}(OH)_{24}$ system as a function of fullereneol concentration in the range of 0.94×10^{-7} to 4.5×10^{-5} mol/L; [dsDNA] = 6.31×10^{-5} mol/L; average standard error, 0.17%.

through fluorescence emission titration of fullereneol. The enhancement of the fluorescence intensity of fullereneol with DNA at increasing concentrations is shown in Figure 4. One can observe that even for nanoscale concentration of DNA the fluorescence intensity of fullereneol increases from 25 to 100 (Figure 4a). The plot in Figure 4b is broken down into two regimes corresponding to ranges from 1.3×10^{-9} to 3.1×10^{-6} g/L and 2.5×10^{-5} to 5×10^{-5} g/L. The low [DNA] range in the plots of Figure 4b (detection limit = 1.3 ng/mL) are close to what can be accomplished with current available fluorescence probes, ie, Hoechst 33258 (20 ng/mL) and YO-PRO-1/YOYO-1 (0.5–2.5 ng/mL). In addition, from the shape and intensity of emission spectrum recorded for [DNA] = 2.1×10^{-9} mol/L (Figure 4a), it is useful to point out that the sensitivity can be extended into lower regions.

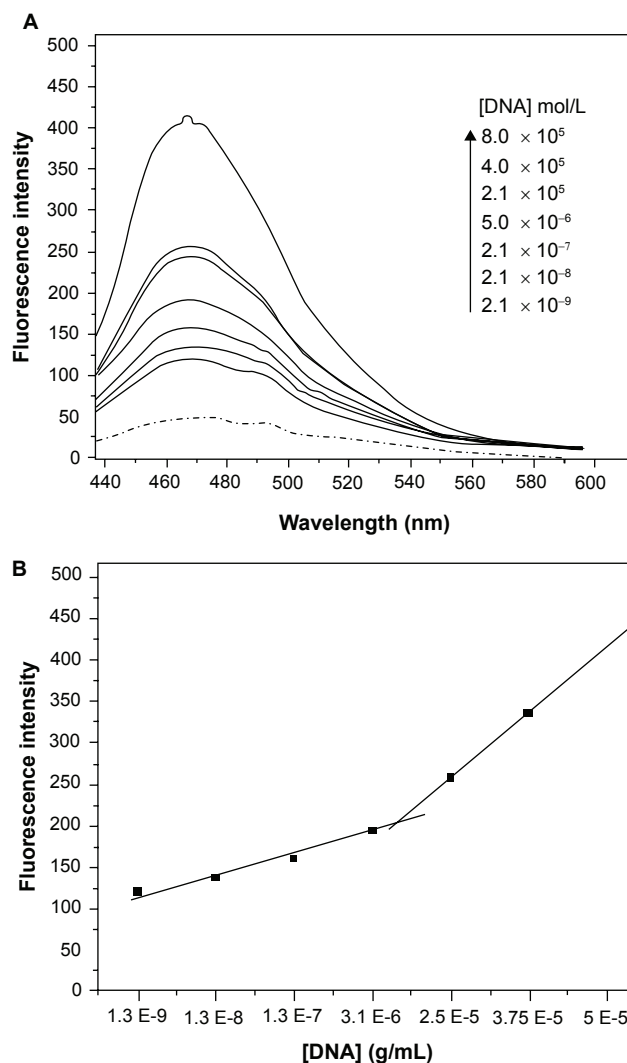


Figure 4 Dependence of fluorescence intensity of $C_{60}(OH)_{24}$ on dsDNA concentration. **A**) Fluorescence spectra of fullereneol (—) with increasing concentration of DNA (---) with excitation at 420 nm; **B**) Plot of fluorescence intensity of fullereneol as a function of [dsDNA] in the concentration range of 1.3×10^{-9} to 4.4×10^{-6} mol/L; [$C_{60}(OH)_{24}$] = 4.5×10^{-5} mol/L; average standard errors: 2.69% for $2.5E^{-5}$ – $5E^{-5}$ region and 10.80% for $1.3E^{-9}$ – $3.1E^{-6}$ region.

As regards the chemical interactions between fullereneol and the DNA target, the electrostatic and intercalative binding are ruled out and hydrogen-bonding interaction can only be taken under consideration. Earlier studies^{38,39} have pointed out that hydrogen-bonding plays the main role in the interaction between fullereneols and proteins. Thus, the major groove binding of fullereneol through the hydrogen-bonding between its hydroxyl groups and free or bridged $-NH_2$ in base-pairs of DNA is predictable.

Taking into account that phenols can interact with phosphates,⁶³ the hydrogen bonding between fullereneol and phosphate backbone of DNA can be also suggested as a possibility for the binding of fullereneols with DNA.

From the linear plot in Figure 3b according to equation (1) the value of n was estimated to be 0.8 ± 0.2 . This value

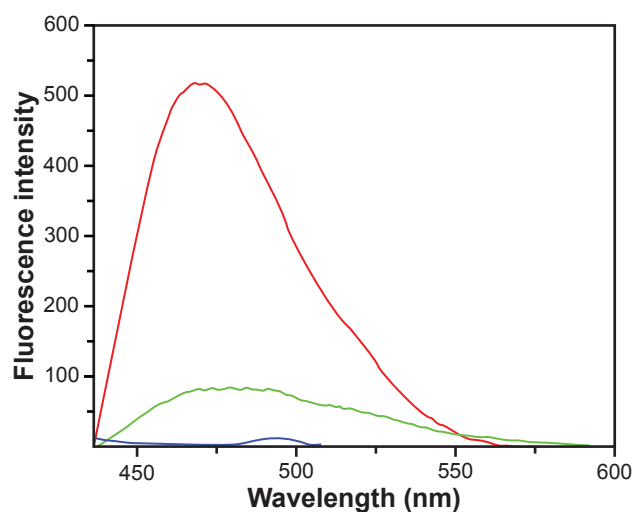


Figure 5 Emission spectra of $C_{60}(OH)_{24}$ (red line), DNA-sodium salt (blue line) and $C_{60}(OH)_{24}$ - DNA-sodium salt complex (green) line.

accounts for a single fullereneol molecule associated with a base pair of DNA. An important question is whether the fullereneol binds significantly to the phosphate backbone of DNA in addition to nonintercalative groove binding to base-pairs of DNA.

Because of its diameter (9.8 Å) the globular three-dimensional $C_{60}(OH)_{24}$ molecule does not fit the minor

groove of DNA (6 Å). The width of the major groove (12 Å) is larger than 9.8 Å and thus the fullereneol molecule can fit snugly according to a nonintercalation model as shown in Scheme 1a.

Indeed, upon binding to sodium salt of DNA (Figure 5), the fluorescence intensity of fullereneol does not increase, but decreases, which suggests that only in the absence of hydrogen bond-forming P-OH moieties of DNA, fullereneol binds to base-pairs into the major groove of DNA, according to a nonintercalative model, which strongly change its average local environment. The perceptible shift of the emission maximum of fullereneol also support a strong change of its average local environment. We can thus conjecture that, under the present experimental conditions with native dsDNA, hydrogen binding to phosphate backbone to the outside of dsDNA helix is the main binding mode of fullereneol $C_{60}(OH)_{24}$ to DNA, as shown in Scheme 1b.

Conclusions

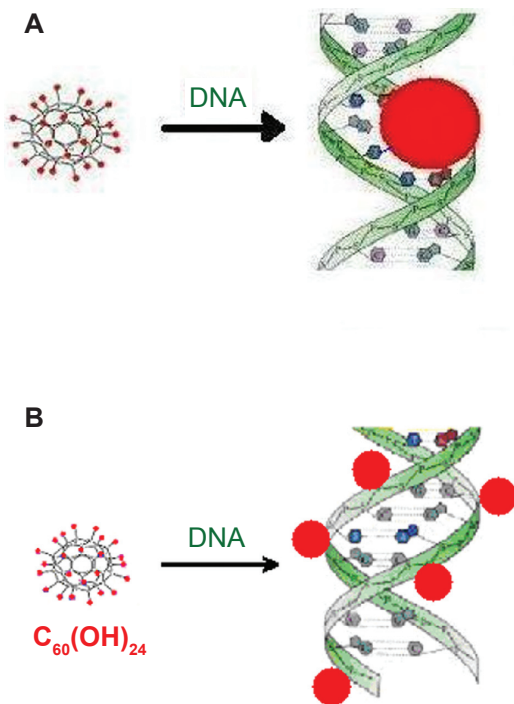
Fullereneol $C_{60}(OH)_{24}$ binds to phosphate backbone to the outside of native dsDNA and to base-pairs within major groove of sodium salt of dsDNA. The fluorescence of fullereneol $C_{60}(OH)_{24}$ is highly enhanced by dsDNA due to the binding of the probe to DNA in a nonintercalative way. Because of its high binding affinity ($K = 10^5 M^{-1}$) and sensitivity ($1.2 \times 10^{-9} g/mL$) towards DNA, there are good prospects that $C_{60}(OH)_{24}$ will be used as versatile fluorescent probe for DNA quantification. In addition to its high sensitivity, other advantages of this fullereneol-based method include its simplicity, nontoxicity, and rapidity.

Acknowledgments

We are grateful to the Romanian Ministry of Education and Research for funding through the CNCSIS-GRANT Nr.306. The authors report no conflicts of interest in this work.

References

1. Wilkinson JM. Nanotechnology applications in medicine. *Med Device Technol.* 2003;14:29–31.
2. Roco MC. Nanotechnology: convergence with modern biology and medicine. *Curr Opin Biotechnol.* 2003;14:337–346.
3. Tong R, Cheng J. Anticancer polymeric nanomedicines. *Polymer Review.* 2007;47:345–381.
4. Moghimi SM, Theme editor and T. Kissel T. Particulate nanomedicines. *Adv Drug Deliv Rev.* 2006;58:1451–1455.
5. Torchilin VP. Targeted pharmaceutical nanocarriers for cancer therapy and imaging. *AAPS J.* 2007;9:E128–E147.
6. Chan WCW. *Bio-applications of Nanoparticles.* New York, NY: Springer Science; 2007.
7. Lammers T, Hennink WE, Storm G. Tumor-targeted nanomedicines: principles and practice. *Br J Cancer.* 2008;99:392–397.



Scheme 1 Binding fullereneol $C_{60}(OH)_{24}$ to dsDNA. **A)** Binding fullereneol to the major groove of sodium salt of dsDNA. **B)** Binding fullereneol to the outside of the dsDNA.

8. Muthu MS, Singh S. Targeted nanomedicines: effective treatment modalities for cancer, AIDS and brain disorders. *Nanomed*. 2009;4:105–118.
9. Kreuter J. Nanoparticulate systems for brain delivery of drugs. *Adv Drug Deliv Rev*. 2001;47:65–81.
10. Da Ros T. Twenty years of promises: Fullerenes in medicinal chemistry In: Cataldo F, Da Ros T, editors. *Medicinal Chemistry and Pharmacological Potential of Fullerenes and Carbon Nanotubes*. New York, NY: Springer-Verlag; 2008.
11. Injac R, Radic N, Govedarica B, Dvordjevic A, Borut S. Bioapplication and activity of fullereneol $C_{60}(OH)_{24}$. *Afr J Biotech*. 2008;7:4940–4950.
12. Yamawaki H, Iwai N. Cytotoxicity of water-soluble fullerene in vascular endothelial cells. *Am J Physiol Cell Physiol*. 2006;290:1495–1502.
13. Cui D. Medicinal chemistry and pharmacological potential of fullerenes and carbon nanotubes. In: Cataldo F, Da Ros T, editors. *Functionalized Carbon Nanotubes and their Applications*. New York, NY: Springer-Verlag; 2008.
14. Beuerle F, Lebovutz R, Hirsch A. In: Antioxidant properties of water-soluble fullerene derivatives. Cataldo F, Da Ros T, editors. *Medicinal Chemistry and Pharmacological Potential of Fullerenes and Carbon Nanotubes*. New York, NY: Springer-Verlag; 2008.
15. Bosi S, Da Ros T, Spalluto G, Balzarini J, Prato M. Synthesis and anti-HIV properties of new water-soluble bis-functionalized $[C_{60}]$ fullerene derivatives. *Bioorg Med Chem Lett*. 2003;13:4437–4440.
16. Nakamura E, Isobe M. Functionalized fullerenes in water. The first 10 years of their chemistry, biology, and nanoscience. *ACC Chem Res*. 2003;36:807–815.
17. Bosi S, Da Ros T, Spalluto G, Prato M. Fullerene derivatives: an attractive tool for biological applications. *Eur J Med Chem*. 2003;38:913–923.
18. Satoh M, Takayanagi I. Pharmacological studies on fullerene C_{60} , a novel carbon allotrope, and its derivatives. *J Pharmacol Sci*. 2006;100:513–518.
19. Lai HS, Chen Y, Chen WJ, et al. Free radical scavenging activity of fullereneol on grafts after small bowel transplantation in dogs. *Transplant Proc*. 2000;32(6):1272–1274.
20. Lai HS, Chen WJ, Chiang LY. Free radical scavenging activity of fullereneol on the ischemia-reperfusion intestine in dogs. *World J Surg*. 2000;24(4):450–454.
21. Wang H, Joseph JA. Quantifying cellular oxidative stress by dichlorofluorescein assay using microplate reader. *Free Radic Biol Med*. 1999;27:612–616.
22. Tsai MC, Chen YH, Chang LY. Polyhydroxylated C_{60} Fullereneol, a novel free-radical trapper, prevented hydrogen peroxide – and cumene hydroperoxide – elicited changes in rat hippocampus in-vitro. *J Pharm Pharmacol*. 1997;49:438–454.
23. Chiang LY, Lu FJ, Lin JW. Free radical scavenging activity of water-soluble fullereneols. *J Chem Soc Chem Commun*. 1995;12:1283–1286.
24. Jin H, Chen WQ, Tanh XW, et al. Polyhydroxylated C_{60} fullereneols, as glutamate receptor antagonists and neuroprotective agents. *J Neurosci Res*. 2000;62:600–607.
25. Gelderman MP, Simakova O, Clogston JD, et al. Adverse effects of fullerenes on endothelial cells: Fullereneol $C_{60}(OH)_{24}$ induced tissue factor and ICAM-1 membrane expression and apoptosis in vitro. *Int J Nanomedicine*. 2008;3:59–68.
26. Huang HC, Lu LH, Chiang LY. Antiproliferative effect of polyhydroxylated C_{60} on vascular smooth muscle cells. *Proc Electrochem Soc*. 1996;403:96–100.
27. Zhao QF, Zhu Y, Ran TC, et al. Cytotoxicity of fullereneols on *Tetrahymena pyriformis*. *Nucl Sci Techniq*. 2006;17:280–284.
28. Silva GA. Neuroscience nanotechnology: progress, opportunities and challenges. *Nat Rev Neurosci*. 2006;7:65–74.
29. Silva GA. Nanotechnology approaches for the regeneration and neuroprotection of the central nervous system. *Surg Neurol*. 2005;63:301–306.
30. Dugan LL, Lovett EG, Quick KL, Latharius J, Lin TT, O'Malley KL. Fullerene-based antioxidants and neurodegenerative disorders. *Parkinsonism Relat Disord*. 2001;7:243–246.
31. Dugan LL, Gabrielsen JK, Yu SP, et al. Buckminsterfullerene free radical scavengers reduce excitotoxic and apoptotic death of cultured cortical neurons. *Neurobiol Dis*. 1996;3:129–135.
32. Injac R, Radic N, Govedarica B, et al. Acute doxorubicin pulmototoxicity in rats with malignant neoplasm is effectively treated with fullereneol $C_{60}(OH)_{24}$ through inhibition of oxidative stress. *Pharmacol Rep*. 2009;61:335–342.
33. Injac R, Perse M, Cerne M, et al. Protective effects of fullereneol $C_{60}(OH)_{24}$ against doxorubicin-induced cardiotoxicity and hepatotoxicity in rats with colorectal cancer. *Biomaterials*. 2009;30:1184–1196.
34. Injac R, Boskovic M, Perse M, et al. Acute doxorubicin nephrotoxicity in rats with malignant neoplasm can be successfully treated with fullereneol $C_{60}(OH)_{24}$ via suppression of oxidative stress. *Pharmacol Rep*. 2008;60(5):742–749.
35. Yin JJ, Lao F, Meng J, et al. Inhibition of tumor growth by endohedral metallofullerene nanoparticles optimized as reactive oxygen species scavenger. *Mol Pharmacol*. 2008;74:1132–1140.
36. Zhu J, Ji Z, Wang J, et al. Tumor-inhibitory effect and immunomodulatory activity of fullerol $C_{60}(OH)_x$. *Small*. 2008;4(8):1168–1175.
37. Bogdanovi G, Kojic V, Dvordjevic A, Vojinovic M, Baltiv VV. Modulating activity of fullerol $C_{60}(OH)_{24}$ on doxorubicin-induced cytotoxicity. *Toxicol in Vitro*. 2004;18:629–637.
38. Bingshe X, Xuguang L, Xiaoqin Y, Jinli Q, Weijun J. Studies on the interaction of water-soluble fullerenols with BSA and effects of metallic ions. *Mat Res Soc Symp Proc*. 2001;675:W7.4.1–W7.4.5.
39. Zhao GC, Zhang P, Wei XW, Yang ZS. Determination of proteins with fullerol by a resonance light scattering technique. *Anal Biochem*. 2004;334:297–302.
40. Nafisi S, Saboury AA, Keramat N, Neault J-F, Tajmir-Riahi HA. Stability and structural features of DNA intercalation with ethidium bromide, acridine orange and methyleneblue. *J Molec Struct*. 2007;827:35–43.
41. Heller DP, Greenstock CL. Fluorescence lifetime analysis of DNA intercalated ethidium bromide and quenching by free dye. *Biophys Chem*. 1994;50:305–312.
42. Le Pecq JB, Paoletti C. A new fluorometric method for RNA and DNA determination. *Anal Biochem*. 1966;17:100–107.
43. Nishioka T, Yuan J, Matsumoto K. Fluorescent lanthanide labels with time-resolved fluorometry in DNA analysis. In: Ferrari M, editor. *Micro/Nano Technology for Genomic and Proteomics*. New York, NY: Springer-Verlag; 2007.
44. Kubát P, Lang K, Zelinger Z, Král V. Formation of lanthanide(III) texaphyrin complexes with DNA controlled by the size of the central metal cation. *J Inorg Biochem*. 2005;99:1670–1675.
45. Selvin PR. Principles and biophysical applications of lanthanide-based probes. *Annu Rev Biophys Biomol Struct*. 2002;31:275–302.
46. Lakowicz JR. *Principles of Fluorescence Spectroscopy*. New York, NY: Springer-Verlag; 2006. p. 681–697.
47. Gao F, Chao H, Zhou F, Yuan YX, Peng B, Jin LN. DNA interactions of a functionalized ruthenium(II) mixed-polypyridyl complex $[Ru(bpy)2ppd]^{2+}$. *J Inorg Biochem*. 2006;100:1487–1494.
48. Song G, Li L, Liu L, et al. Fluorometric determination of DNA using a new ruthenium complex $Ru(bpy)2PIP(V)$ as a nucleic acid probe. *Anal Chem*. 2002;18:757–759.
49. Zipper H, Brunner H, Bernhagen J, Vitzhum F. Investigations of DNA interaction and surface binding by SYBR Green I, its structure determination and methodological implications. *Nucleic Acids Res*. 2004;32:e103.
50. Rengarajan K, Cristol SM, Mehta M, Nickerson JM. Quantifying DNA concentration using fluorometry: a comparison of phluorophores. *Mol Vis*. 2002;8:416–421.
51. Vitzhum G, Geiger H, Bisswanger H, Brunne J, Bernhagen J. A quantitative fluorescence based microplate assay for the determination of double-stranded DNA using SYBR Green I a standard ultraviolet trans-illuminator gel imaging system. *Anal Biochem*. 1999;276:59–64.
52. Cui D. Advances and prospects on biomolecular functionalized carbon nanotubes *J Nanosci Nanotechnol*. 2007;17:1298–1314.

53. Wei W, Sethuraman A, Jin AC, Monteiro-Riviere NA, Narayan RJ. Biological properties of carbon nanotubes. *J Nanosci Nanotechnol*. 2007;7:1284–1297.
54. Star A, Tu E, Niemann J, Gabriel J, Joiner CS, Valcke C. Label-free detection of DNA hybridization using carbon nanotube network field-effect transitions. *Proc Nat Acad Sci U S A*. 2006;103:921–926.
55. Hobbie EK, Bauer BJ, Stephens J, Becker ML, McGuiggan P, Hudson SD. Colloidal particles coated and stabilized by DNA-wrapped carbon nanotubes. *Langmuir*. 2005;21:10284–10287.
56. Chiang LY, Upasani RB, Swirczewski SS. Evidence of hemiketals incorporated in the structure of fullerols derived from aqueous acid chemistry. *J Am Chem Soc*. 1993;115:5453–5457.
57. Schneider NS, Darwish AD, Kroto HW, Taylor R, Walton DRM. *J Chem Soc Chem Commun*. 1994;4:463–464.
58. Chiang LY, Upasani RB, Swirczewski SS. Versatile nitronium chemistry for C_{60} fullerene functionalization. *J Am Chem Soc*. 1992;114:10154–10157.
59. Alves GC, Ladeira LO, Righi A, et al. Synthesis of $C_{60}(OH)_{18-20}$ in aqueous alkaline solution under O_2 -atmosphere. *J Braz Chem Soc*. 2006;17:1186–1190.
60. Husebo LO, Sitharaman B, Furukawa K, Kato TJ, Wilson LJ. Fullerenols revisited as stable radical anions. *J Am Chem Soc*. 2004;126:12055–12064.
61. Djordjevic A, Vojinovic-Miloradiv M, Petranovic N, Devcerski A, Bogdanovic GJ, Adamov J. Synthesis and characterization of water-soluble biologically active $C_{60}(OH)_{24}$. *Arch Oncol*. 1997;5:139–145.
62. Troshin PA, Astakova AS, Lyubovskaya RN. Synthesis of fullereneols from halofullerenes. *Fullerenes Nanotubes Carbon Nanostruct*. 2005;13:1–13.
63. De Vente J, Bruyn PJ, Zaagsma J. Fluorescence spectroscopic analysis of the hydrogen bonding properties of catecholamines, resorcinolamines, and related compounds with phosphate and other anionic species in aqueous solution. *J Pharm Pharmacol*. 1981;33:290–296.

International Journal of Nanomedicine

Dovepress

Publish your work in this journal

The International Journal of Nanomedicine is an international, peer-reviewed journal focusing on the application of nanotechnology in diagnostics, therapeutics, and drug delivery systems throughout the biomedical field. This journal is indexed on PubMed Central, MedLine, CAS, SciSearch®, Current Contents®/Clinical Medicine,

Submit your manuscript here: <http://www.dovepress.com/international-journal-of-nanomedicine-journal>

Journal Citation Reports/Science Edition, EMBase, Scopus and the Elsevier Bibliographic databases. The manuscript management system is completely online and includes a very quick and fair peer-review system, which is all easy to use. Visit <http://www.dovepress.com/testimonials.php> to read real quotes from published authors.